SWC 2019
Air conditioning system with cascaded integration of a latent heat storage for flexible and efficient operation

Timo Korth, Felix Loistl, Christian Schweigler

CENERGIE Research Center Energy-efficient Buildings and Districts
Munich University of Applied Sciences, Department of Building Services Engineering,
Lothstr. 34, 80335 Munich, Germany
timo.korth@hm.edu

Abstract

A novel concept for the integration of latent heat storages in the refrigerant cycle of air conditioning systems is presented. A pilot installation of a VRF system (variable refrigerant flow) to verify the performance of the system is under preparation. The latent heat storage (LHS) is in direct heat exchange with an evaporating or condensing refrigerant flow. Thus, temperature losses by an intermediate heat carrier loop are eliminated. Furthermore the integration of the storage shall not affect the evaporation and condensation level of the air conditioning system in order to keep the energetic efficiency of the system unchanged. During loading the LHS is cooled by evaporation of refrigerant in parallel with two indoor units, allowing for system operation at standard suction pressure. During unloading the storage serves as a condenser, connected in series between the two indoor units. In this phase air-conditioning is continued, while action of the compressor is reduced to 50% load, approximately. Energy flows and efficiency are discussed for the different phases of the cycle.

Keywords: Thermal storage, Latent heat storage, Phase change material, PCM, Air conditioning, VRF-System

1. Introduction

The increased use of renewable energy sources leads to a growing demand for storage systems facilitating an efficient and consistent use of these energies. In the field of heating and cooling applications huge potential is seen in latent heat storages (LHS). The new approach which is presented in this paper comprises loading and unloading of the LHS by means of direct heat exchange with the refrigerant. The concept shall be applied for a Variable-Refrigerant-Flow heating and cooling system (VRF-System) which is driven by the electricity output of a PV generator. In VRF systems which directly act on the supply air flow no secondary heat carrier is available for integration of a heat or cold storage. Thus, a thermal storage in direct contact to the refrigerant cycle offers a straightforward solution with minimal technical complexity.

The characteristics of latent heat storage are described in detail by Dincer and Rosen (2011), starting from the thermodynamic, kinetic, chemical, technical and economic criteria and ending up with several case studies. Furthermore (Hauer et al. 2013) and (Mehling and Cabeza 2008) present a detailed characterization of Phase Change Materials (PCM) and give an overview of different design concepts for latent heat storages. In this field, several investigations focus on the research of phase change materials with different phase change temperatures aiming at a characterization and realistic modeling of the process to optimize the design of the storages (Frazzica et al., 2017), (Fan et al., 2016), (Palomba et al., 2017), (Oro et all 2012). In these studies a heat carrier fluid is used to charge and discharge the storage. Up to now, loading and unloading of the latent heat storages by direct heat exchange with the refrigerant is not a common technical concept. As a first implementation an air-source heat pump system with a latent heat storage supporting the defrost mode of the heat pump has been developed and introduced into the market (Daikin). By this means, inversion of the refrigeration cycle in defrost mode is avoided, allowing for continuous operation of the heat pump and increased heating comfort.

In this publication, a concept for activating alatent heat storage by direct heat exchange with the refrigerant supporting the output of useful heating or cooling is presented and analyzed. The development offers increased flexibility of operation, allowing for high energetic efficiency and intelligent interaction with the grid.

doi:10.18086/swc.2019.22.03 Available at http://proceedings.ises.org

2. System concept: Air-conditioning system with latent heat storage

A novel concept of integrating the storage directly into the refrigerant cycle is proposed. Key aspect is the impact on pressure and temperature levels of the refrigerant cycle induced by conventional heat storage concepts. As a characteristic feature of the concept, the loading and unloading processes of the LHS take place through direct evaporation and direct condensation of refrigerant in the heat exchanger embedded in the storage, respectively. The novel aspect of the proposed configuration is given by separation of the evaporator component in two parts and by switching of the hydraulic interconnection of the components: The loading process is realized in parallel connection of the two evaporator units (EU) and the LHS which allows a loading of the storage at the nominal evaporation temperature. To use the stored thermal energy with the provided temperature level of the storage, during unloading a serial flow of the refrigerant through the evaporator units and the LHS is established, providing almost full capacity of the refrigeration system with substantially reduced operation of the compressor (Korth et al, 2019b). Fig. 1 shows the loading process of the storage (left) and unloading process of the storage (right) in the log(p)-h diagram. The loading process can be described by the following steps:

1-2 Compression of the refrigerant vapor by the compressor
2-3 Condensation of the refrigerant with heat rejection to the environment in the condenser unit
3-4 Expansion of the refrigerant through the three parallel expansion valves to evaporation pressure
4-1 Evaporation of the refrigerant in parallel in both evaporator sections and in the LHS by absorption of heat from the room and by heat extraction from the LHS, resulting in a crystallization of the PCM.

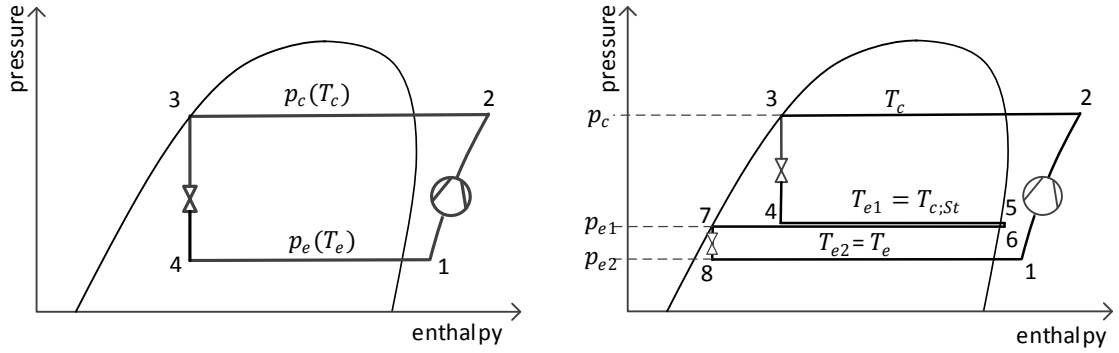

Fig. 1: The loading process of the storage (left) and unloading process of the storage (right) in the log(p)-h diagram.

During the unloading process the following steps take place:

1-2 Compression of the refrigerant vapor by the compressor
2-3 Condensation of the refrigerant in the condenser unit with heat rejection to the environment
3-4 Expansion of the refrigerant in the expansion valve to evaporation pressure p_{e1} of EU1.
4-5 Evaporation of the refrigerant with heat absorption from the room in EU1.
6-7 Condensation of the refrigerant with heat rejection into the LHS on the same pressure level (T_{e1}=$T_{c;St}$) assuming that no pressure drops occur within the internal cycle.
7-8 Control of the refrigerant flow rate, avoiding retention of liquid refrigerant in the LHS.
8-1 Evaporation of the refrigerant with heat absorption from the room in EU2 at standard evaporation temperature of the system (T_{e2} = T_e)

3. Air-conditioning system for validation of the concept

For validation of the proposed system concept, an air conditioning system based on a commercial VRF multi-split system for heating and cooling is installed. For the ease of continuous laboratory investigation a novel system type has been chosen, allowing installation of all system components inside the building. For this purpose the compressor unit and outdoor heat exchanger are installed inside the building with air ducts providing connection to the ambient air (Daikin 2018). Serving as a model system for development of the cascaded latent heat storage integration, the following VRF system configuration has been chosen: One

outdoor unit with a nominal heating and cooling capacity of 14 kW, three indoor units with a nominal cooling capacity of 3,6 kW and a nominal heating capacity of 4 kW. For the analysis of the operation the following measurement equipment is installed:

- 10 Pt100 temperature sensors
- 4 pressure gauges with 0,1% accuracy
- 4 differential pressure gauges with 0,05 % accuracy
- 2 Mass flow sensors (Coriolis flow meter)

Fig. 2 shows a simplified flow scheme of the system in cooling mode with the position of the sensors. The evaporating units EU1 and EU2 are supplied by one refrigerant line but can also be run independently. In addition, the storage can be implemented in between these units to realize the above concept for the integration of the storage. This requires an additional interconnection and a liquid receiver avoiding transfer of gaseous refrigerant and providing a separation of pressure between the pair EU1/LHS and the following evaporator unit EU2. The evaporating unit EU3 serves as a reference unit and is supplied independently with refrigerant from the compressor (in heating mode) or the condenser unit (in cooling mode), respectively. As usual in VRF systems, the liquid refrigerant is subcooled by an additional heat exchanger ("Subcooler") in the core (compressor) unit in order to avoid flashing of the refrigerant along the distributed piping of the system. The subcooling effect is provided by evaporation of a small quantity of refrigerant which is extracted from the main refrigerant cycle. Apart from the temperature sensors and absolute pressure gauges, the differential pressure gauges shall allow a precise analysis of the operation, in particular the separation of the pressure levels in EU1, LHS and EU2. The thermal design of the latent heat storage is governed by the intended mode of use: If the system shall allow peak shaving, the LHS shall provide approximately 50% of the capacity of the indoor units for a period of a few hours. Consequently, the thermal design aims at a thermal duty of about 4 kW providing a thermal content of 7,2 kWh.

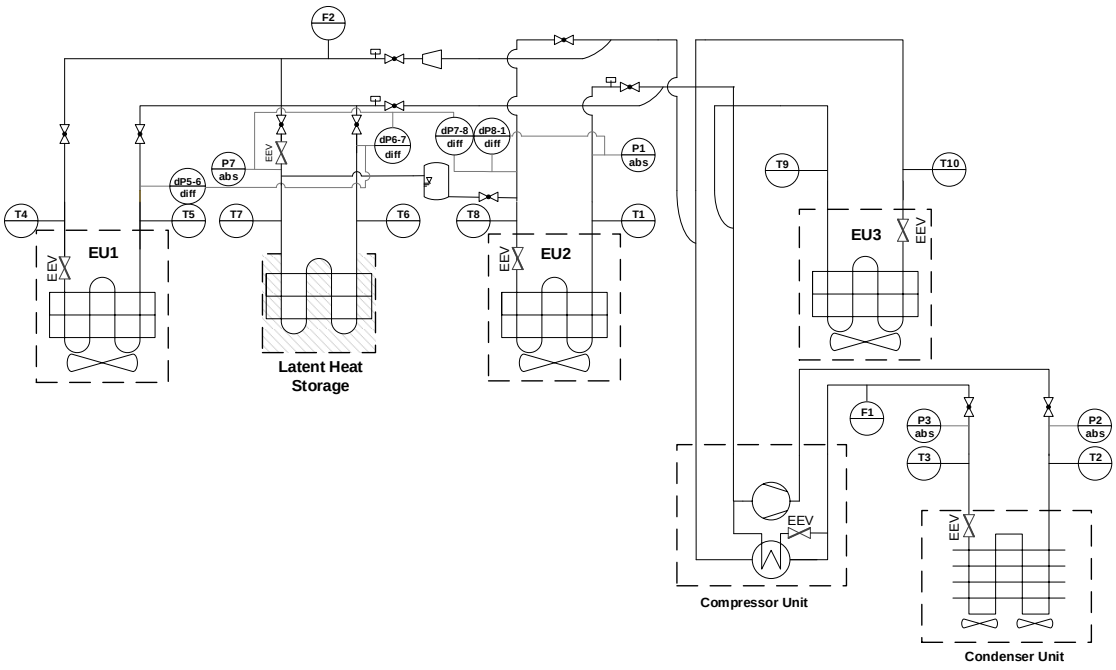

Fig. 2: Simplified flow scheme of the VRVi System with latent heat storage in cooling mode.

4. Cycle analysis and theoretical model for the reference system

To analyze and characterize the reference system a physical simulation model of the air conditioning system has been set up in the Software Engineering Equation Solver (EES). The aim is the description of the steady state of the cycle. This model is the basis for further investigations concerning the integration of the LHS in the refrigerant cycle. The heat exchangers are modeled based on UA-values and logarithmic mean temperature difference. In the calculation model, the evaporating units are divided into two sections, taking into account evaporation and superheating of the refrigerant. The condensing unit is covered by an overall

UA-value. For determination of the compressor work an isentropic coefficient is applied. The input parameters include the basic information, i.e. the boundary conditions, of the refrigerant cycle, obtained from the operation of the real installation. Table 1 lists values of selected parameters of the system operating in a steady state under typical conditions.

Table 1: Selected parameters out of experimental data of the reference system operating in a steady state.

Pressure in bar		Temperature in °C					
p_e	p_c	T_e	T_c	T_{Room}	$T_{ambient}$	$T_{EU1;Air\ out}$	$T_{CU1;Air\ out}$
9,1	22,7	4,1	37,3	23,9	28,8	11,3	38,7
Refr. mass flow in kg/s		Capacity in W					Efficiency
$\dot{m}_{total}$	$\dot{m}_{EU1}$	$\dot{Q}_{EU1}$	$\dot{Q}_{EU2}$	$\dot{Q}_{EU3}$	$\dot{Q}_{CU}$	P_{Comp}	EER
0,061	0,018	3464	3494	3464	12485	2012	5,2

5. Simulation model: Operation of the latent heat storage

The analysis of the system performance with latent heat storage integrated in the reference system (as described in section 2) is realized on basis of the simulation model described in section 4. All input parameters are taken from the reference operation (Table 1), while the phase change temperature is set to 10 °C. For the storage characterization a validated one-dimensional simulation model is used (Korth et. al 2019a). The calculation models of the reference air conditioning system and the LHS are linked and a full storage cycle consisting of the loading and unloading process is analyzed in comparison to the operation without the storage (see Table 1). Due to the innovative nature of the system configuration with cascaded integration of the LHS, for the integral concept no further validation with reference to literature data can be given.

Thermal model of the latent heat storage

The calculation model of the latent heat storage incorporates the growth of the crystallized zone within the PCM volume coupled with direct evaporation of refrigerant inside the heat exchanger tubes passing through the storage. For the crystallization of the PCM an ideal radial propagation of the phase front is assumed, starting from the refrigerant tubes passing through the volume of the LHS. As result, a time dependent heat resistance $R_{PCM(t)}$ for thermal conduction across the storage material is obtained. Finally, the time-dependent overall thermal resistance $R_{total,St}(\mathrm{t})$ for the heat transfer between the LHS and the refrigerant inside the tubes is calculated by equation 1, taking into account the evaporation of the refrigerant inside the tube (R_{ref}), and thermal conduction across the tube wall (R_{tube}) and in the PCM volume ($R_{PCM}(t)$). By equation 2, a relation between the time-dependent diameter $d_{PCM}(\mathrm{t})$ of the crystallized cylindrical PCM zone and the current state of charge (SOC) is given. When the storage volume is completely liquid (SOC=0), the phase front coincides with the outer surface of the tube ($d_{PCM}(t)=d_{tube,o}$); when the storage is fully solidified (SOC=1) the maximum diameter of the cristallized PCM volume is attained ($d_{PCM}(t)=d_{PCM,max}$).

$$R_{total,St}(\mathrm{t}) = R_{ref} + R_{tube} + R_{PCM}(\mathrm{t}) = \frac{1}{\alpha_{ref} \cdot A_{tube,i}} + \frac{\ln \frac{d_{tube,o}}{d_{tube,i}}}{\pi \cdot L_{tube} \cdot 2 \cdot \lambda_{tube}} + \frac{\ln \frac{d_{PCM}(t)}{d_{tube,o}}}{\pi \cdot L \cdot 2 \cdot \lambda_{PCM,eff}} \quad \text{(eq.1)}$$

$$d_{PCM}(\mathrm{t}) = \left(\left({d_{PCM,max}}^2 - {d_{tube,o}}^2 \right) \cdot \mathrm{SOC}(\mathrm{t}) + {d_{tube,o}}^2 \right)^{0,5} \quad \text{(eq. 2)}$$

Loading of the storage

In loading mode the LHS is connected in parallel to the evaporation units EU1, EU2 and EU3. By

evaporation of the refrigerant in the heat exchanger of the storage heat is extracted from the LHS. Finally, the phase change material is completely solidified. The evaporation takes place at the nominal evaporation pressure, given by the suction pressure of the compressor. Fig. 3 shows the process in the log(p)h-diagram (full line, blue) in comparison to the reference operation (dotted line, red). The condensing pressure rises as a consequence of the additional cooling demand of the storage that has to be released by the condensing unit. This temperature increase is at a maximum at the beginning of the loading process and follows a decreasing trend according to the decreasing capacity of the LHS over the course of time. As a consequence the specific enthalpy difference of the evaporation (state points 1 to 3, blue full line) decreases. That results in an increase of the refrigerant mass flow at EU1, EU2 and EU3 for a constant cooling capacity. In addition, an extra amount of refrigerant is required for operation of the LHS. To meet these requirements the compressor capacity rises. In total, the overall system efficiency represented by the EER decreases. A quantitative analysis is given in the following sections.

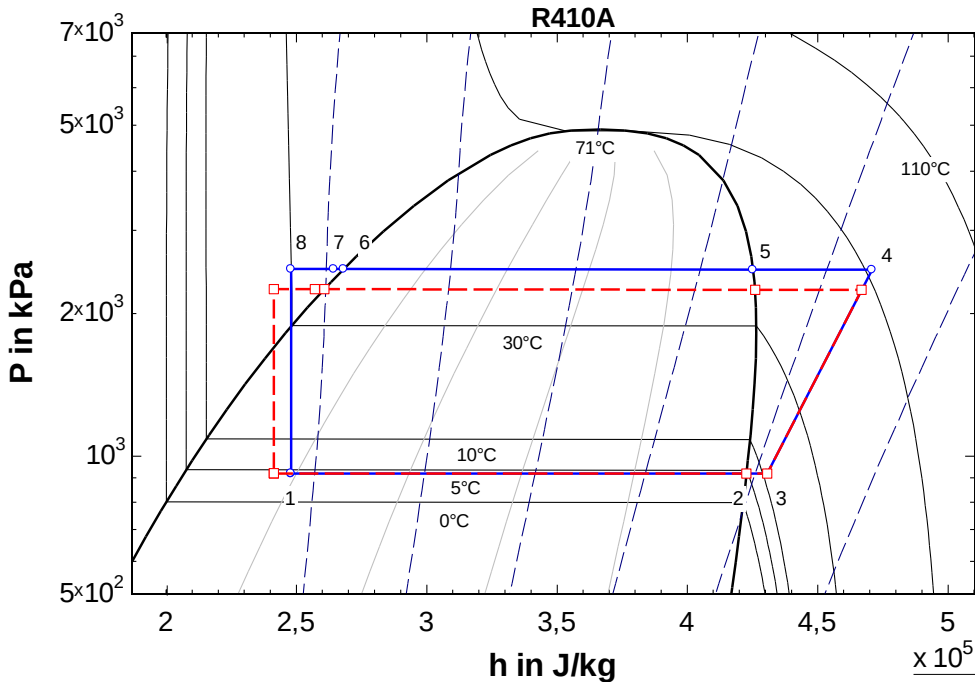

Fig. 3: Refrigerant cycle in the log(p)h-diagram (refrigerant: R410a) in normal operation (dotted line, red, steady state) and during loading of the storage (full line, blue, state points at the beginning of the process).

Unloading of the storage

In unloading mode, the LHS is integrated in the serial interconnection EU1-LHS-EU2, while EU3 operates in parallel to this sub-system (see section 2). In this mode, refrigerant flow through the EU1-LHS-EU2 subsystem is controlled by only one expansion valve at the inlet to EU1. Controlled variable is the refrigerant superheat at the outlet of EU2. During condensation of the refrigerant in the heat exchanger of the storage, heat is absorbed by the PCM resulting in a phase change from solid to liquid. This condensation takes place at a medium pressure level. Fig. 4 shows the process in the log(p)h-diagram, again in comparison to the reference operation (dotted line, red). In this case the condensation temperature can be decreased because the storage absorbs a certain amount of heat, providing a reduction of the heat duty of the condenser. This temperature decrease is valid for the whole unloading process.

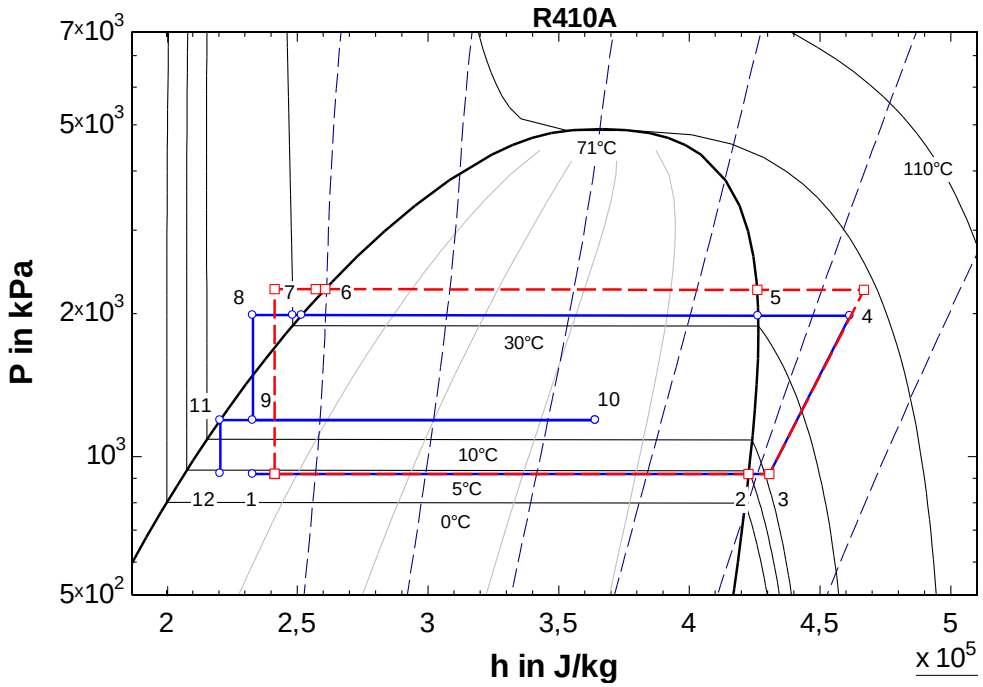

Fig. 4: Refrigerant cycle in the log(p)h-diagram (refrigerant: R410a) during unloading of the storage in cascaded configuration (state points at the end of the process).

During unloading, again a characteristic decrease of the storage capacity occurs, influencing the operation of EU1 (state points 9 to 10, blue full line). With falling capacity, a growing fraction of the refrigerant remains in liquid state at the outlet of EU1, resulting in a decrease of the specific enthalpy and the vapor quality (from about x=0,95 to x = 0,7) at state point 10. Furthermore, due to the increasing thermal resistance the condensation pressure in the storage and thereby the evaporation pressure in EU1 rises slightly over the course of time. Both aspects result in a capacity decrease of EU1. This is discussed in detail below. As a consequence of the storage operation, a higher specific enthalpy difference is provided to EU2 (state points 12 to 3) as compared to the reference situation without storage. Thus for operation at unchanged external operating conditions and constant cooling capacity, a lower refrigerant mass flow is passing through EU2. Due to the lower condensation level in comparison to the reference cycle, EU3 also operates with a higher specific enthalpy difference (state points 1 to 3), resulting in a decrease of the refrigerant mass flow to meet the required cooling capacity. In total, during unloading of the LHS the overall refrigerant mass flow is decisively decreased, providing a substantial decrease of the compressor capacity. As a benefit of the contribution of the LHS, which covers a part of the cooling load, in this phase the overall system efficiency represented by the EER is increased. Of course, for a fair comparison a complete cycle – comprising loading and unloading of the storage – has to be taken into account, as described below.

As a proof for the cycle analysis given above, Fig. 5 presents the temporal profiles of the thermal capacity, the refrigerant mass flow, the compressor capacity and the EER. Thereby a full storage cycle is taken into account. In addition, each diagram shows the reference state given by the system operating without storage at steady state, as given in Table 1. The thermal capacities $\dot{Q}_{EU2}$ and $\dot{Q}_{EU3}$ (top left) show an almost constant trend according to the reference state, while $\dot{Q}_{EU1}$shows a constant trend during the loading process (0:00h to 1:27h), followed by a decreasing trend during unloading of the storage (1:27h to 4:01h). The trend of the storage capacity $\dot{Q}_{LHS}$ can be divided into three phases: a constant beginning for about 20 minutes, followed by a strong decrease until the end of the loading (at 1:27h) and a rather constant capacity during unloading (1:27h to 4:01h). The overall integral of the storage capacity equals zero, due to the assumption of negligible thermal losses. The constant trend at the beginning is a result of the limitation of the refrigerant mass flow by the selection of the expansion valve. Simultaneously, excessively high capacities of the storage are avoided, which might induce an overload situation for the entire refrigeration system.

During unloading, EU1 and LHS interact directly. Thus, the decreasing trend of $\dot{Q}_{EU1}$ during unloading of the storage perfectly reflects the decrease of the storage capacity.

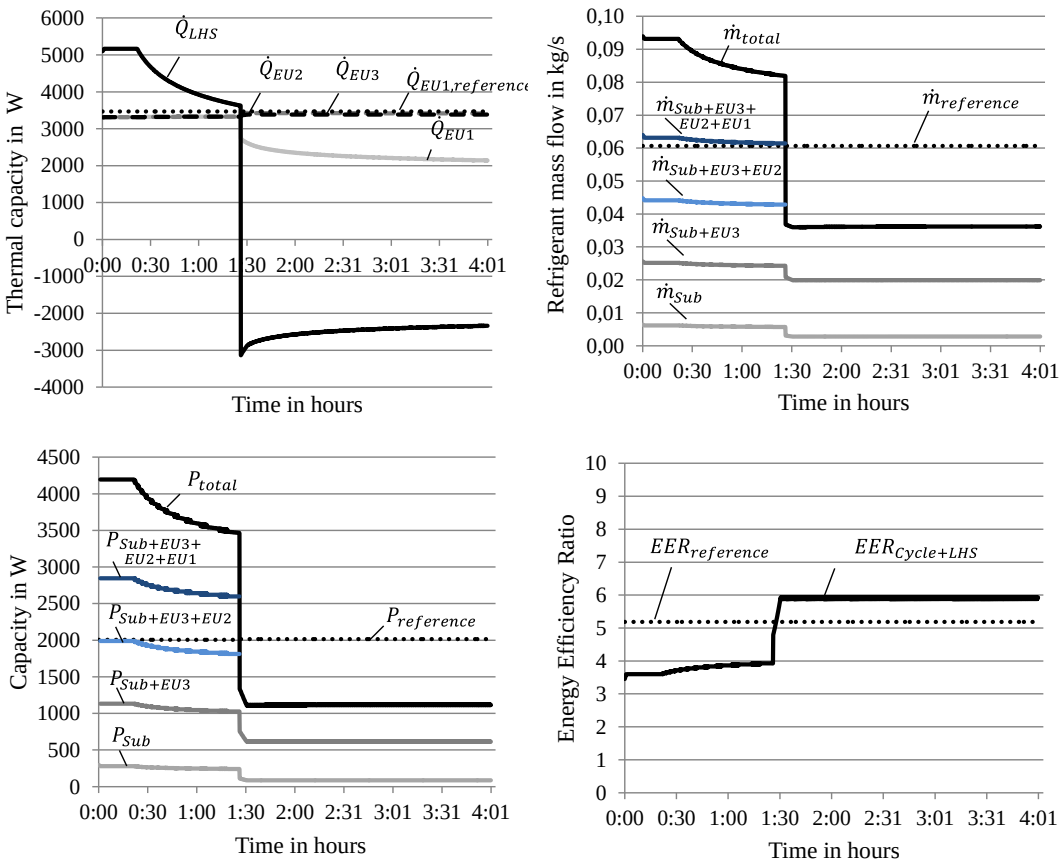

Fig. 5: Analysis of a full storage cycle: Thermal capacity, refrigerant mass flow (accumulated), compressor capacity (accumulated) and EER each plotted against the time. The loading process starts at 0:00 and ends at 1:25 h, while the unloading process lasts from 1:27 h to 4:01 h.

The refrigerant mass flow diagram (top right) emphasizes that the mass flow $\dot{m}_{Sub+EU3+EU2+EU1}$ of the standard system is increased versus $\dot{m}_{reference}$, when the LHS is loaded in parallel to the operation of the evaporator units (EU). This is a result of the increase of the condensing pressure during the loading process and the related decrease of the specific enthalpy difference at the evaporator units (EU), as discussed earlier. $\dot{m}_{Sub}$ represents the refrigerant mass flow used for subcooling of the refrigerant before leaving the core (compressor) unit. The total refrigerant mass flow $\dot{m}_{total}$ is obtained by adding the flow through the LHS.

During unloading of the storage, the overall refrigerant mass flow $\dot{m}_{total}$ is almost halved. This is mainly a result of the serial interconnection providing a contribution of the LHS to the total cooling output of the system. In addition, a slight decrease of the mass flow through EU3 is visible, resulting from the increased specific enthalpy difference at the evaporator units. The reduction of the overall mass flow also affects the subcooler heat exchanger positively.

The profile of the compressor capacity (bottom left) shows a clear congruence with the refrigerant mass flow. It is obvious that the loading process of the LHS requires more capacity P_{total}while the unloading process needs less capacity input, in agreement with the refrigerant mass flow processed in the different phases of the cycle. Moreover it is elucidated that the increase of the condensation pressure level has a decisive negative influence on the efficiency by increasing the compressor capacity ($P_{Sub+EU3+EU2+EU1}$ vs. $P_{reference}$).

The overall efficiency is illustrated in Fig. 5 (bottom right), based on the following definition of the $EER_{Cycle+LHS}$:

$$EER_{Cycle+LHS} = \frac{\dot{Q}_{EU1} + \dot{Q}_{EU2} + \dot{Q}_{EU3} + \dot{Q}_{LHS}}{P_{el}} \qquad \text{(eq. 3)}$$

For this definition, the cooling effect stored in the LHS and provided by the LHS during loading and unloading, respectively, is integrated in the overall balance. Thus, the heat duties regarded for the determination of the EER do not reflect the current supply of cooling to the user. Rather, this definition describes the cycle efficiency of a vapor compression cycle for the operating conditions of the cycle during operation with LHS, i.e. modified pressure levels of evaporation and condensation and modified specific enthalpy differences induced by the integration of the LHS, as discussed above.
The loading process starts with an $EER_{Cylce+LHS}$ value that is 1,3 less than $EER_{reference}$, following an increasing trend. This is in agreement with the decrease of the condensing pressure throughout the loading process of the LHS. The constantly higher $EER_{Cycle+LHS}$ during unloading of the storage results from the lowered condensing pressure.
Fig. 6 contrasts the reference air conditioning system (AC-System) without LHS and the AC-System with LHS by comparing the overall compressor energy (left) and the cooling energy (right). For this comparison, only the useful output of the system is taken into account, i.e. only the useful cooling provided by the evaporator units (EU) during loading (1:27 h) and unloading of the LHS (2:34 h) is integrated over the time.

As a result of this analysis an effective EER is defined, characterizing the performance of the system by the cumulated energy balance, covering a complete operational cycle.

$$EER_{AC-System+LHS} = \frac{\int(\dot{Q}_{EU1} + \dot{Q}_{EU2} + \dot{Q}_{EU3})\ dt}{\int P_{el}\, dt} \qquad \text{(eq. 4)}$$

In total, for the same operating conditions the VRF system with LHS requires slightly more compressor energy compared to the reference AC-system, providing a little less cooling energy. The effective EER is calculated to $EER_{AC-System+LHS} = 4{,}6$ compared to the systems efficiency of $EER_{reference} = 5{,}2$. Thus, a slightly negative effect of the usage of the storage in terms of energy efficiency of the system is found. Yet, on the other hand the configuration with thermal storage offers flexibility for improved interaction with the electric grid or utilization of beneficial ambient conditions.

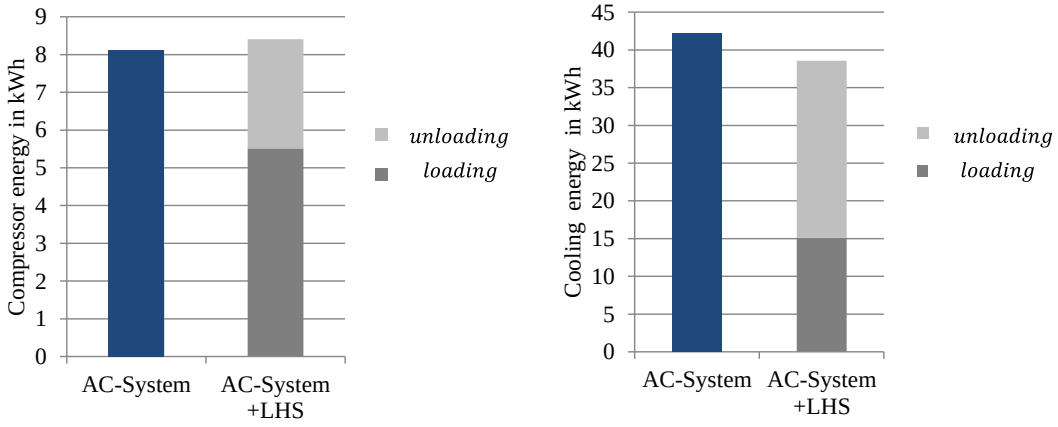

Fig. 6: Overall compressor energy (left) and overall cooling energy (right) for the standard AC system and the system with LHS (with contribution of the loading and unloading phase).

Analysis of the storage operation

To analyze the heat transfer process during loading and unloading of the latent heat storage Fig. 7 shows the UA values, thermal capacities and temperatures, each plotted against the state of charge (SOC) of the LHS.

During the loading process, evaporation of the refrigerant at temperature T_e in the heat exchanger of the LHS is driven by heat transfer from the PCM with phase change temperature T_{PCM} (cf. Fig. 7 bottom left). In this phase heat is extracted from the PCM volume. Due to the increase of the thickness of the solidified PCM layer, the thermal resistance increases substantially, resulting in a strong influence on the temporal profile of the heat transfer.

The unloading process is composed of heat extraction from the room by evaporation of the refrigerant in the evaporation unit 1(Fig. 7 bottom left: $T_{e;EU1}$ against T_{Room}) linked with condensation of the refrigerant vapor

in the LHS, driven by heat absorption by the melting PCM (Fig. 7 bottom left: $T_{c;LHS}$ against T_{PCM}).

For both cases, loading and unloading of the LHS, a strong decrease of the UA value for the heat exchange between refrigerant and PCM volume is found (cf. Fig. 7 top, right), given by the increasing thermal resistance of the PCM layer in solid or liquid state, respectively. Yet, this temporal behavior is not equally reflected by the profiles of the thermal capacity of the storage during loading and unloading, as shown in Fig. 7 (top, right). This difference can be explained by analyzing the complete heat transfer process in both phases, as shown in Fig. 8 and Fig. 9.

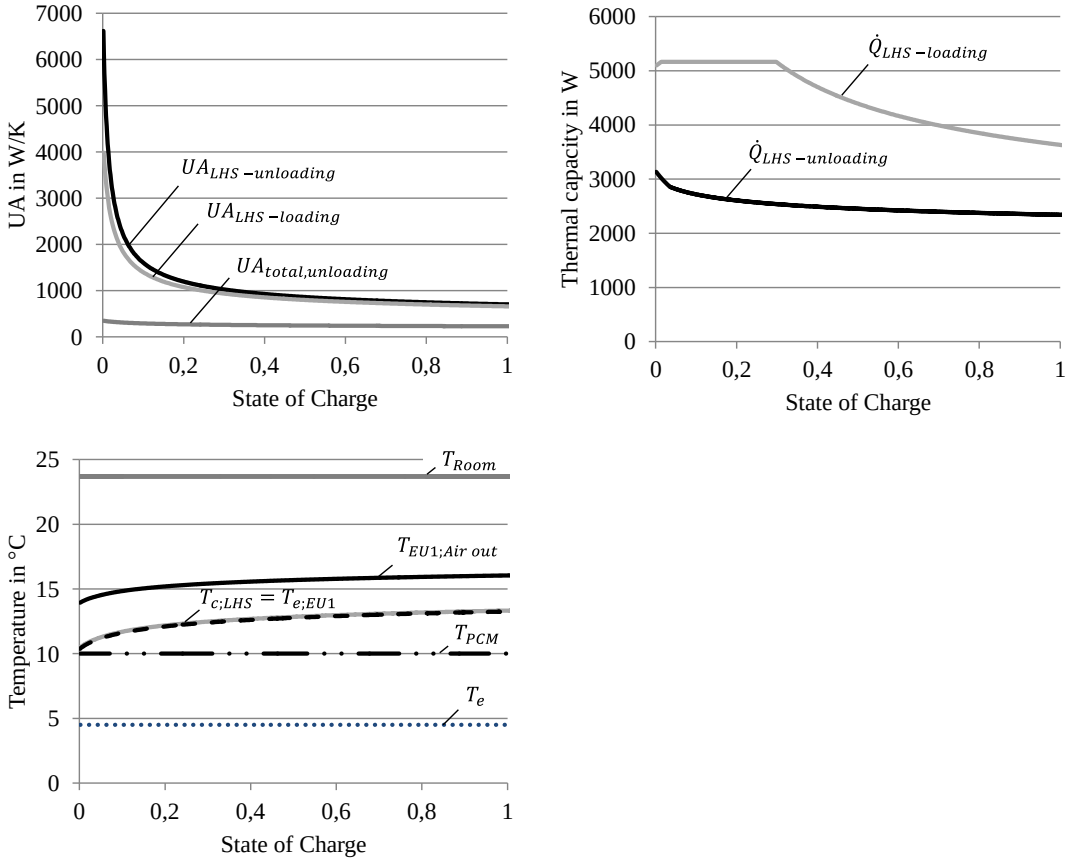

Fig. 7: Characterization of the LHS: UA values, thermal capacities, temperatures each plotted against the state of charge (SOC).

In Fig. 8 and Fig. 9 the thermal resistance (left) and driving temperature difference for the processes are displayed. The loading process (Fig. 8) is characterized by operation with constant driving temperature difference between PCM and refrigerant and a strong increase of the thermal resistance of the PCM layer $R_{totel:\,refrigerant\,(evaporation)-PCM}$ by a about 500%. Consequently, a strong decrease of the thermal capacity occurs during this phase. During unloading (Fig. 9) a cascaded heat transfer from room air, via refrigerant to the PCM takes place. Again, a strong increase of the thermal resistance $R_{refrigerant\,(condenstion)-PCM}$ of the increasing PCM layer is found. Yet, the overall heat transfer is dominated by the thermal resistance between room air and refrigerant $R_{air-refrigerant\,(evaporation)}$. The later stays constant during the unloading phase, resulting in an only moderate increase of the total thermal resistance between room air and LHS R_{total} by about 50%. As a consequence of the reduced heat transfer, the heat extraction from the room air decreases, resulting in increasing air outlet temperatures leaving the evaporator unit EU1 which is serially coupled with the LHS. Thus, the mean air temperature, given as an average of the inlet and outlet temperature passing through the EU1 increases, providing a positive effect for the overall heat transfer from room air to the PCM volume in the LHS. This trend of increasing driving temperature difference to some extent counterbalances the increase of the thermal resistance, resulting in an only moderate decrease of the thermal capacity of the LHS during unloading. In total a rather strong temporal change of the thermal capacity is found for the

loading process, while the unloading process with two-stage heat transfer from room air to the LHS exhibits an only moderate decrease of the capacity.

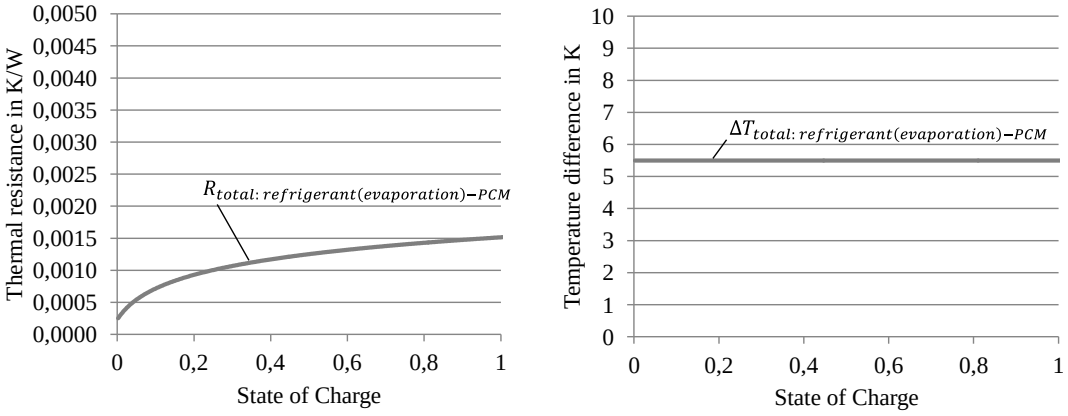

Fig. 8: Loading process of the LHS: Thermal resistance and temperature difference plotted against the state of charge (SOC).

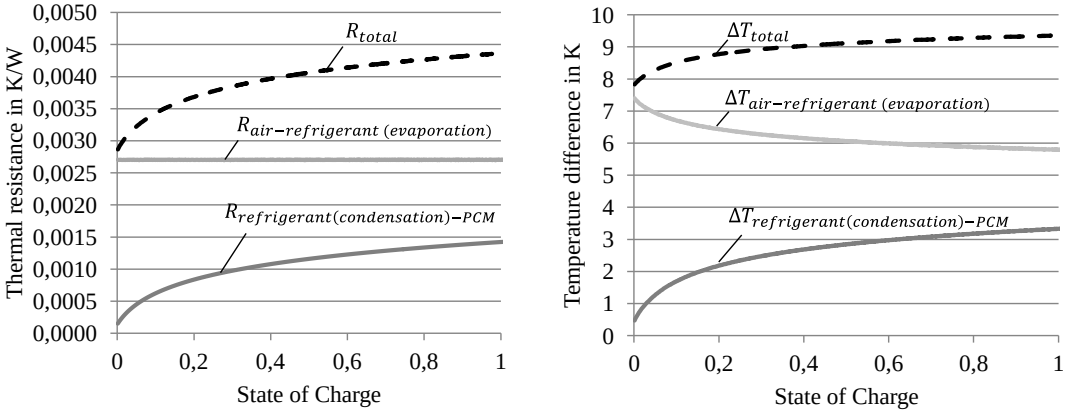

Fig. 9: Unloading process of the LHS: Thermal resistances and temperature differences plotted against the state of charge (SOC).

6. Conclusion

A novel concept for the integration of latent heat storages (LHS) in the refrigerant cycle of air conditioning systems is analyzed in relation to system operation without LHS under same conditions. Information about the performance of the reference system has been gained by analysis of the operation of a pilot installation of a VRF system. The off-the-shelf multi-split system is equipped by comprehensive measurement for detailed analysis of the system performance. According to the novel concept, the latent heat storage is directly integrated into the refrigerant cycle, forming a cascaded configuration with two evaporator units. The underlying heat transfer processes are analyzed with regard to driving temperature differences and thermal resistances. In the unloading phase, the cascaded interconnection of the LHS leads to an attenuated decrease of the storage capacity in comparison to the characteristic behavior of latent heat storages coupled to a water-based heat carrier. The novel concept aims at increased flexibility of the air-conditioning system. By integration of the thermal storage, consumption of driving energy from the grid and provision of useful cooling can be decoupled, offering positive effects for the stability of the grid and improved utilization of renewable energy sources. In addition, the temporal flexibility offers the potential to operate the system at favorable ambient conditions with increased energetic efficiency.

As expected, under standard operation conditions the integration of the storage has a slightly negative effect on the energy efficiency of the system. However, a clear advantage over conventional concepts of storage integration is expected in terms of energy efficiency. This will be demonstrated by further analysis.

7. ACKNOWLEDGEMENTS

This work has been conducted within the research project "SolarSplit", funded by the German Federal Ministry for Economic Affairs and Energy (FKZ 0325900B).

NOMENCLATURE

d	diameter in m
$\dot{m}$	Refrigerant mass flow (kg/s)
p	pressure (bar)
P	compressor capacity
$\dot{Q}$	thermal capacity (W)
R	thermal resistance (K/W)
T	temperature (°C)
ΔT	temperature difference (K)

Indices

c	condensation
e	evaporation
LHS	Latent heat storage
ref	refrigerant

8. References

Dincer, I., Rosen, M.A., 2011. Thermal Energy Storage – System and applications, Second Edition, John Wiley & Sons, West Sussex, United Kingdom

Daikin, 2017. VRV IV i-series. VRV IV heat pumps for indoor installation

Fan, L., Zhu, Z., Xiao, S., Liu, M., Lu, L., Zeng, Y., Yu, Z., Cen,K., An experimental and numerical investigation of constrained melting heat transfer of a phase change material in a circumferentially finned spherical capsule for thermal energy storage, Applied Thermal Engineering, 2016

Frazzica, A., Palomba, V., La Rosa, D., Brancato, V., Experimental comparison of two heat exchanger concepts for latent heat storage applications, IRES, Düsseldorf 2017

Hauer, A., Hiebler, S., Reuß, M., 2013. Wärmespeicher, 5., vollständig überarbeitete Auflage, Fraunhofer IRB Verlag, Karlsruhe

Korth, T., Loistl, F., Krönauer, A., Storch, A., Schex, R., Schweigler, C, 2019a. Capacity enhancement of air conditioning systems by direct integration of a latent heat storage, Applied Thermal Engineering, DOI 10.1016/j.applthermaleng.2019.114727

Korth, T., Loistl, F., Schweigler, C., 2019. Novel integration of latent heat storage in multi-split air conditioning systems. Intl. Congress of Refrigeration, Montreal, 2019b, to be published.

Loistl, F., Korth, T., Schweigler, C., 2016. Einsatz von Latentwärmespeichern in Klimageräten, DKV-Tagung, Kassel

Mehling, Harald, Cabeza, Luisa F., 2008. Heat and cold storage with PCM – An up to date introduction into basics and applications, Springer Verlag, Heidelberg

Oro, E., Gil, A.,Miró, L., Peiró, G., Alvarez, S., Cabezza, L.Thermal Energy Storage Implementation Using Phase Change Materials for Solar Cooling and Refrigeration Applications, Energy Procedia 30 (2012) 947 – 956

Palomba, V., Frazzica, A., Brancato, V., Experimental investigation of a latent heat storage for solar cooling applications, Applied Energy 2017